Iranian Journal of Pharmaceutical Sciences
Spring 2008: 4(2): 141-148
www.ijps.ir

Original Article

Bioresorbability Evaluation of Hydroxyapatite Nanopowders in a Stimulated Body Fluid Medium

Arash Hanifi*, Mohammad Hossein Fathi

Department of Materials Science, Isfahan University of Technology, Isfahan, Iran

Abstract

The bone mineral consists of tiny hydroxyapatite (HA) crystals in the nanoregime. Nanostructured HA is also expected to have better bioactivity than coarser crystals. This paper reports on the *in vitro* evaluation of bone like HA nanopowders. The prepared HA nanopowder was characterized for its phase purity, chemical homogeneity and bioactivity. Fourier transform infrared (FT-IR) spectroscopy was used to identify the functional groups. X-ray diffraction analysis was carried out to study the phase composition. The *in vitro* test was performed in a stimulated body fluid medium. The changes in the pH of SBF medium were measured at pre-determined time intervals using a pH meter. The dissolution of calcium ions in the SBF medium was determined by an atomic absorption spectrometer. FT-IR spectroscopy result combined with the X-ray diffraction exhibited single phase of HA with carbonate peaks in the FT-IR spectrum. Results indicated that increasing the sintering temperature increases the crystallinity and the crystallite size of HA nanopowders. HA nanopowders ionic dissolution rate was found to be quite higher than conventional HA and closer to biological apatite owing to its nanostructure dimensions.

Keywords: Bioresorbability; Hydroxyapatite; Nanostructure.
Received: December 18, 2007; *Accepted:* March 15, 2008

1. Introduction

The stoichiometric hydroxyapatite (HA) is biocompatible, bioactive i.e. ability to form a direct chemical bond with living tissues, osteoconductive, non-toxic, non-inflammatory and non-immunogenic agent [1-3]. The use of conventional HA in the form of thin film, powder, dense or porous blocks is abundance at microscale level [4, 5]. Microscale HA is typically a highly stable phase i.e. less bioresorbable, which is an undesirable characteristic because it impedes the rate of bone regeneration when used as a bone substitute [6]. It is desirable that the hydroxyapatite used for implants fabricating be bioresorbable so that it can be replaced over a period of time, with regenerated bone upon implantation. The resorbability of HA can be improved with making its crystallinity degree similar to biological HA (60-70%) and reducing its grain size to nano-level [7].

The recent trend in bioceramic research is

*Coressponding author: Arash Hanifi, Department of Materials Science, Isfahan University of Technology, Isfahan, 84156-83111, Iran.
Tel (+98)311-3912750, Fax (+98)311-3912752
E-mail: a.hanifi@gmail.com

focused on overcoming the limitations of calcium phosphates, precisely HA ceramics and in improving their biological properties via exploring the unique advantages of nanotechnology. It has been also recorded that the resorption process of synthetic HA (conventional forms) is quite different from that of bone mineral. Bone mineral crystals are in nano sizes with a very large surface area. These crystals are grown in an organic matrix and have very loose crystal-to-crystal bonds. Therefore, the resorption by osteoclasts is quite homogeneous. HA (micron size), on the contrary, presents a low surface area and have strong crystal-to-crystal bond. In addition, the bone mineral present a higher bioactivity compared with synthetic HA [8].

Engineering HA at nano levels would have amazing functional properties due to its grain size, large surface area to volume ratio and ultrafine structure similar to biological apatite, which would have a great impact on implant-cell interaction in the body environment [9].

It has been claimed that the behavior of the HA family upon immersion in a simulated body fluid (SBF) is structure and composition-dependent [10]. The powders' dissolution rate is dependent largely on the crystallinity level, phase composition, microstructure, surface area and density [11-13]. The *in vitro* and in vivo Ca^{2+} ion release from the synthetic HA nanopowders is similar to that for bone apatite and significantly faster than this for microscale conventional HA. Therefore, it is becoming important to develop HA nanopowders with precise control of particle size, morphology, crystallinity degree and chemical composition [4].

Keeping the above points in view, present study was aimed to produce synthetic HA nanopowders with superior bioresorption and the evaluation of their *in vitro* behavior.

2. Material and methods

2.1. Synthesis of hydroxyapatite nanopowders

The synthesis procedure of HA nanopowders was discussed in a previous work [14]. In brief, a stoichiometric amount of calcium nitrate tetrahydrate ($Ca(NO_3)_2.4H_2O$, Merck) and phosphoric pentoxide (P_2O_5, Merck) were used with the molar ratio of 10:3, which is the desired Ca/P ratio observed in HA. Absolute ethanol (C_2H_5OH, Merck) was used as the solvent. The as-prepared solution after dissolving the above precursors slowly is transformed into a gel form after a period of 24 h under continuous stirring at ambient temperature. As-formed gel was aged for 24 h, and then dried in an oven at 80 °C in air for 24 h. The dried gel was sintered at a rate of 5 °C/min. up to 600 °C in a muffle furnace, and finally placed in air for cooling to ambient temperature. To find the effect of sintering temperature on the crystallinity and crystallite size of products, sintering process was also performed in temperatures of 700, 800 and 900 °C.

2.2. Characterization

Fourier transform infrared (FT-IR) spectroscopy (Bomem, MB 100) was used to identify the functional groups. The spectrum was recorded in the 4000-400 cm^{-1} region with 2 cm^{-1} resolution.

The crystallographic structural analysis was carried out by X-ray diffraction (XRD) method using a Philips X'Pert-MPD system powder diffractometer with monochromatic Cu Kα radiation over the 2θ range of 20-80° at a scan rate of 0.02. The peak broadening of XRD reflection can be used to estimate the crystallite size in a direction perpendicular to the crystallographic plane based on Scherrer's formula as Equation (1) [15];

$$Xs=0.9\lambda/(FWHM \times \cos\theta) \quad \text{Equation (1)}$$

Where Xs is the crystallite size [nm], λ the wavelength of X-ray beam (λ=0.15406 nm for CuKα radiation), FWHM the full width at half maximum for the diffraction peak under consideration [rad], and θ the diffraction angle [°]. The diffraction peak at 2θ=26.04° was

chosen for calculation of the crystallite size since it is sharper and isolated from others. This peak assigns to (002) Miller's plane family and shows the crystal growth along the c-axis of the hydroxyapatite crystalline structure.

The fraction of crystalline phase (Xc) in the HA powders can be evaluated by the Equation (2) [16]:

$Xc=1-(V_{112/300}/I_{300})$ Equation (2)

Where I_{300} is the intensity of (300) diffraction peak and $V_{112/300}$ is the intensity of the hollow between (112) and (300) diffraction peaks of HA.

SBF was used to prove the similarity between *in vitro* and *in vivo* behavior of certain bioceramic compositions [17]. Therefore, *in vitro* bioresorbability test was performed in a SBF medium of pH 7.4 at a ratio of 1 mg/ml in a water bath at 37 °C. The SBF medium consists of 9 g NaCl, 5 g KCl and 0.2 g $MgHPO_4.3.H_2O$/L [7]. The changes in the pH of SBF medium were measured at pre-determined time intervals (0 to 14 days) using a pH meter. The dissolution of calcium ions in the SBF medium was determined by an atomic absorption spectrometer (AAS).

3. Results and discussion

The FT-IR spectra of HA sample sintered at 600 °C are shown in Figure 1. The representative FT-IR spectrum, showing all characteristic absorption peaks of pure or stoichiometric HA. The first indication for the formation of HA is in the form of broad FT-IR band centered at about 1000-1100 cm^{-1} [18]. The bands at 960-965 and at 565-601 cm^{-1} correspond to n1 and n4 symmetric P-O stretching vibration of the PO_4^{3-} ion, respectively [19, 20].

The bone contains carbonated HA having 4-6% carbonate by weight, called dahllite [21]. A common method of determining the type of carbonated substitution is to examine the positions of carbonate bands observed in FT-IR spectra [22, 23]. The characteristic bands from inorganic carbonate ion (1465-1415 and 876 cm^{-1}) [17] are present in the FT-IR spectra of HA sample heated at 600 °C. The band at 876 cm^{-1} indicate n2 mode of CO_3^{2-} group or HPO_4 group. This mode, if attributed to carbonate as indicated earlier by Emerson *et al*. [24] and Elliott *et al*. [25], suggest a B-type carbonate substitution i.e., part of the PO_4 (B-type) groups in the apatitic structure were replaced by CO_3^{2-} groups. The HA powder in this study presented carbonate bands at 1462, 1418, and 876 cm^{-1}, which is in agreement with the study of Tinti and co-workers as type B substitution, whereas type A bands locate at 1550, 1457, and 880 cm^{-1} [23]. The bands assigned to the stretching modes of hydroxyl groups (OH) in the HA (3571 cm^{-1}, 632 and 474 cm^{-1}) [17, 18] are clearly observed in the spectra. Thus, according to the stretching frequencies observed and the similarity of the FT-IR spectra of the investigated samples, the possible formation of crystalline carbonated HA by sol-gel synthesis routes could be

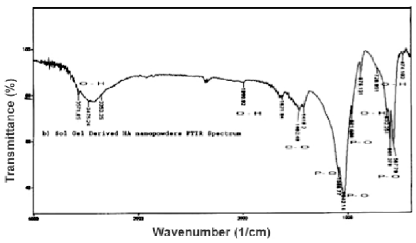

Figure 1. FT-IR spectra of hydroxyapatite sample sintered at 600 °C.

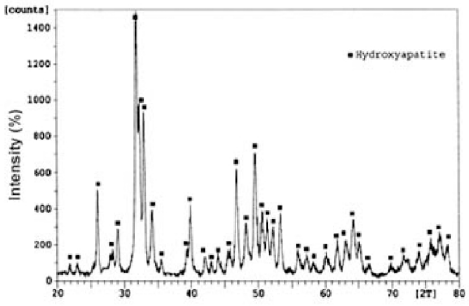

Figure 2. XRD pattern of the hydroxyapatite nanopowders sintered at 600 °C.

suggested.

Figure 2 shows the XRD pattern of HA nanopowders sintered at 600 °C. The result shows a poor crystalline nature of typical apatite crystal structure with broad diffracted peaks and does not show any extraneous phases, which suggests that the sol-gel process has produced phase pure and homogeneous HA. It is also noticed that the crystallographic behavior of HA resembles to that of XRD pattern of biological apatite [26]. The synthesized HA nanopowders are similar in structure with naturally occurring bone apatite with respect to degree of crystallinity and structural morphology.

The XRD spectra of products prepared at different sintering temperatures are shown in Figure 3. Broad diffraction peaks were observed for the all of the powders. Crystalline HA appears to form after the heat-treatment at 600 °C. The CaO phase observed after heat-treatment at 700 °C corresponds to the product of the decomposition of calcium nitrate that remains either partially reacted or unreacted in the gel after heat-treatment at 700 °C.

Figure 3 demonstrates that the sintering temperature plays an important role on the formation of HA. As the sintering temperature is increased from 600 to 900 °C, several of the HA lines become more distinct at higher temperatures, and also the widths of the lines become more narrow, which suggests an increase in the crystallinity degree. It can also be seen that additional crystalline phases (β-TCP) appear at 700 °C, and no other crystalline phase presents besides HA at 600°C. It could be concluded that HA could be decomposed into β-TCP and CaO as the sintering temperature is at 700 °C or above.

The evaluated degrees of crystallinity for these samples are given in the Table 1. It was noticed that the increase of the crystallinity with temperature was not linear. Bouyer *et al*. reported a similar phenomenon [27]. The resorption property of calcium phosphates depends on Ca/P ratio, degree of crystallinity and crystal structure. A remarkable property of the synthetic HA is its bioactivity, in particular the ability, e.g. after implantation, to form chemical bonding with surrounding hard tissues [2, 3]. However, most synthetic apatites are formed via high temperature processes (e.g. sintering), resulting in a well-crystallized structure, which has little or no activity towards bioresorption. This is in contrast to nanocrystalline or bio-crystal apatites, which are typically non-stoichiometric, and which typically exhibit much higher degree of bioactivity. Therefore, the use of sol-gel processes for synthesis of HA became an important research objective [28]. The poorly crystalline apatite structure that obtained in this study is expected to be more active in metabolic activity than the fully developed crystalline HA structure which is considered to be nonsoluble in physiological environment [29].

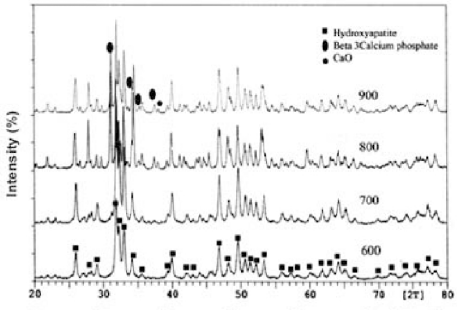

Figure 3. Phase composition of the samples sintered at different temperature of 600, 700, 800 and 900 °C.

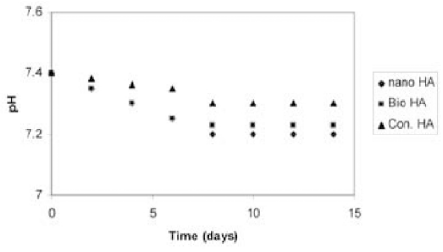

Figure 4. pH changes of HA, bio HA and conventional HA samples.

Table 1. Effect of synthesis temperature on the crystallinity and crystallite size of hydroxyapatite nanopowders.

Sintering temperature (°C)	Crystallinity Xc (%)	Crystallite size Xs (nm±SD)
600	61	20±2
700	73	23±1
800	78	30±3
900	85	34±2

The calculated Xs for the HA powders synthesized at different temperatures based on the diffraction peak using Scherrer's formula is also listed in Table 1. The crystallite sizes of the HA powders were smaller than 50 nm and an increase in crystallite size of the HA powders with the increase of synthetic temperature was observed, i.e. the higher of the synthetic temperature, the larger of the crystallite size of the HA nanopowders formed.

Figure 4 shows a graph of pH versus time which illustrates the resorbability of HA nanopowders. The graph also shows the variation in pH with time for a conventional HA and biological HA for comparison.

Addition of apatite has relatively alkaline effect on the pH of the medium. The pH of the conventional HA was found to be of insignificant variation trend as it was not resorbed in the medium, which indicates its physiological stability during the period of study. But the HA nanopowder showed drastic changes in the pH, suggesting that it dissolves much faster than conventional HA. The pH value is dependent on solubility or resorbability of the HA, wherein the pH decreases as the solubility increases. Accordingly, it is clear from the graph that the rate of bioresorbability of the HA nanopowders is higher than conventional HA and close to biological apatite.

The release of calcium ions from the HA nanopowders was quantitatively estimated to support its *in vitro* bioresorbability (Figure 5). The results show that more calcium ions are released from the HA nanopowders as compared to conventional HA, which may be due to degradation of the HA nanopowders. The amount of calcium release from the HA nanopowders corroborates well with the calcium release pattern of biological apatite. Hence, it can be concluded that the ionic dissolution of HA nanopowders is much similar to that of natural bone mineral *in vitro*. By this way, resorbability of HA can be promoted by engineering the particle size to nano/submicron level.

4. Conclusions

The present work described *in vitro* evaluation of HA nanopowders. It's crystallographic and chemical functionalities are quite similar to biological apatite. The crystallinity of the HA nanoparticles are dependent on the synthetic temperature. The crystallinity and crystallite size of the HA nanoparticles increase with the increase of synthetic temperature. The carbonated HA nanoparticles with low crystallinity show good *in vitro* behavior. The *in vitro* bioresorbability of the HA nanopowders is higher than conventional HA and close to biological apatite, which can be attributed to its high surface area owing to nanostructure processing.

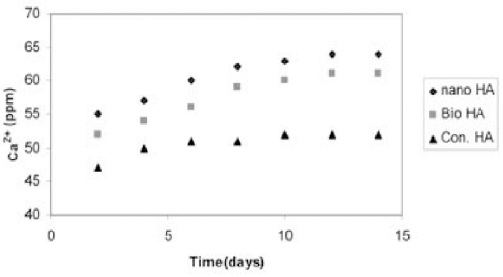

Figure 5. Release of calcium ions from the samples in stimulated body fluid.

Reference

[1] Ducheyne P, Qiu Q. Bioactive ceramics: The effect of surface reactivity on bone formation and bone cell function. *Biomaterials* 1999; 20: 2287-303.

[2] Currey J. Biomaterials: Sacrificial bonds heal bone. *Nature* 2001; 414: 699-708.

[3] Aoki H. *Medical applications of hydroxyapatite*. Tokyo: *Ishiyaku EuroAmerica*, 1994.

[4] Murugan R, Ramakrishna S. Coupling of therapeutic molecules onto surface modified coralline hydroxyapatite. *Biomaterials* 2004; 25: 3073-80.

[5] Murugan R, Rao KP. Grafting of glycidyl methacrylate upon coralline hydroxyapatite in conjugation with demineralized bone matrix using redox initiating system. *Macromolecules* 2003; 11: 14-8.

[6] Kivrak N, Tas AC. Synthesis of calcium hydroxyapatite tricalcium phosphate (HA-TCP) composite bioceramic powders and their sintering behavior. *J Am Ceram Soc* 1998; 81: 2245-52.

[7] Driessens FCM, Boltong MG, De Maeyer EAP, Wenz R, Nies R, Planell JA. The Ca/P range of nanoapatitic calcium phosphate cements. *Biomaterials* 2002; 23: 4011-7.

[8] Kim HM. Ceramic bioactivity and related biomimetic strategy. *Current Opinion Solid State Mater Sci* 2003; 7: 289-99.

[9] LeGeros RZ. *Calcium phosphates in oral biology and medicine*. Basel: Switzerland, Karger A G, 1991; pp. 154-92.

[10] Radin SR, Ducheyne P. The effect of calcium phosphate ceramic composition and structure on *in vitro* behavior, II. Precipitation. *J Biomed Mater Res* 1993; 27: 35-45.

[11] Ducheyne P, Radin S, King L. The effect of calcium phosphate ceramic composition and structure on *in vitro* behavior, I. Dissolution. *J Biomed Mater Res* 1993; 27: 25-34.

[12] Harada Y, Wang JT, Doppalapudi VA, Willis AA, Jasty M, Harris WH, Nagase M, Goldring SR. Differential effects of different forms of hydroxyapatite and hydroxyapatite/tricalcium phosphate particulates on human monocyte/ macrophages *in vitro*. *J Biomed Mater Res* 1996; 31: 19-26.

[13] Wise DL, Trantolo DJ, Lewandrowski KU, Gresser JD, Cattaneo MV, Yaszemski MJ. *Orthopedic, dental and bone graft applications.* Vol. 2. Totowa: Humana Press, 2000.

[14] Fathi MH, Hanifi A. Evaluation and characterization of nanostructure hydroxyapatite powder prepared by sol-gel method. *J Mater Lett* 2007; 61: 3978-83.

[15] Jenkins R, Snyder RL. *Introduction to X-ray powder diffractometry.* New York: John Wiley & Sons, 1996; pp. 123-6.

[16] Landi E, Tampieri A, Celotti G, Sprio S. Densification behaviour and mechanisms of synthetic hydroxyapatites. *J Eur Ceram Soc* 2000; 20: 2377-87.

[17] Ohtsuki C, Kokubo T, Yamamuro. Mechanism of apatite formation on $CaO\text{-}SiO_2\text{-}P_2O_5$ glasses in a simulated body fluid. *J Non-Cryst Solids* 1992; 143: 84-92.

[18] Varma HK, Babu SS. Synthesis of calcium phosphate bioceramics by citrate gel pyrolysis method. *Ceram Int* 2005; 31: 109-14.

[19] Miyaji F, Kono Y, Suyama Y. Formation and structure of zinc-substituted calcium hydroxyapatite. *Mater Res Bull* 2005; 40: 209-20.

[20] Rehman I, Bonfield W. Characterization of hydroxyapatite and carbonated apatite by photo acoustic FTIR spectroscopy. *J Mater Sci Mater Med* 1997; 8: 1-4.

[21] Sinha A, Ingle A, Munim KR, Vaidya SN, Sharma BP, Bhisey AN. Development of calcium phosphate based bioceramics. *Bull Mater Sci* 2001; 24: 653-7.

[22] Chow LC, Sun L, Hockey B. Properties of nanostructured hydroxyapatite prepared by a spray drying technique. *J Res Inst Stand Technol* 2004; 109: 543-51.

[23] Krajewski A, Mazzocchi M, Buldini PL, Ravaglioli A, Tinti A, Taddei P. Fagnano C. Synthesis of carbonated hydroxyapatite: Efficiency of the substitution and critical evaluation of analytical methods. *J Mol Struct* 2005; 221: 744-7.

[24] Emerson WH, Fischer EE. The infrared absorption spectra of carbonate in calcified tissues. *Arch Oral Biol* 1962; 7: 671-83.

[25] Elliott JC, Holcomb DW, Young RA. Infrared determination of the degree of substitution of hydroxyl by carbonate ions in human dental enamel. *Calcif Tissue Int* 1985; 37: 372-5.

[26] Murugan R, Rao KP, Kumar TSS. Heat-deproteinated xenogeneic bone from slaughterhouse waste: Physico-chemical properties. *Bull Mater Sci* 2003; 26: 523-8.

[27] Bouyer E, Gitzhofer F, Boulos MI. Morphological study of hydroxyapatite nanocrystal suspension. *J Mater Sci Mater Med* 2000; 11: 523-31.

[28] Liu DM, Troczynski T, Tseng WJ. Water-based sol-gel synthesis of hydroxyapatite: Process development. *Biomaterials* 2001; 22: 1721-30.

[29] Kim HM, Kim Y, Park SJ, Rey C, Lee HM, Gimcher MJ, Ko JS. Thin film of low-crystalline calcium phosphate apatite formed at low

temperature. *Biomaterials* 2000; 21: 1129-34.
[30] Posner AS. Crystal chemistry of bone mineral. *Physiol Rev* 1969; 49: 760-92.